



Published in final edited form as:

*Traffic*. 2018 December ; 19(12): 933–945. doi:10.1111/tra.12612.

## Newly Synthesized Polycystin 1 Takes Different Trafficking Pathways to the Apical and Ciliary Membranes

Allison L. Gilder<sup>#1</sup>, Hannah C. Chapin<sup>#1</sup>, Valeria Padovano<sup>1</sup>, Christina L. Hueschen<sup>2</sup>, Vanathy Rajendran<sup>2</sup>, and Michael J. Caplan<sup>1,2,\*\*</sup>

<sup>1</sup>Department of Cell Biology, Yale University School of Medicine P.O. Box 208002., New Haven, CT 06520-8026.

<sup>2</sup>Department of Cellular & Molecular Physiology, Yale University School of Medicine, P.O. Box 208026., New Haven, CT 06520-8026.

# These authors contributed equally to this work.

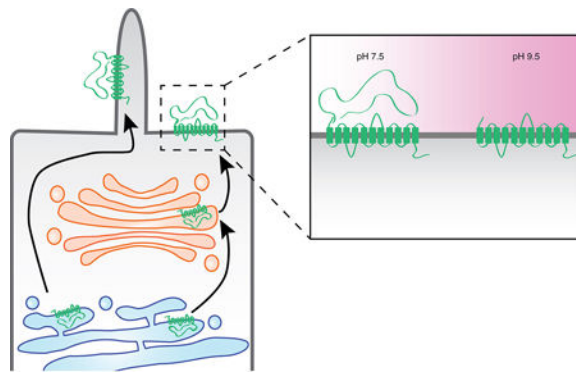
### Abstract

Mutations in the genes encoding polycystin 1 (PC1) and polycystin 2 (PC2) cause Autosomal Dominant Polycystic Kidney Disease (ADPKD). These transmembrane proteins co-localize in the primary cilia of renal epithelial cells, where they may participate in sensory processes. PC1 is also found in the apical membrane when expressed in cultured epithelial cells. PC1 undergoes autocatalytic cleavage, producing an extracellular N-terminal fragment that remains non-covalently attached to the transmembrane C-terminus. Exposing cells to alkaline solutions elutes the N-terminal fragment while the C-terminal fragment is retained in the cell membrane. Utilizing this observation, we developed a “strip-recovery” synchronization protocol to study PC1 trafficking in polarized LLC-PK1 renal epithelial cells. Following alkaline strip, a new cohort of PC1 repopulates the cilia within 30 minutes, while apical delivery of PC1 was not detectable until 3 hours. Brefeldin A blocked apical PC1 delivery, while ciliary delivery of PC1 was Brefeldin A insensitive. Incubating cells at 20°C to block trafficking out of the trans Golgi network also inhibits apical but not ciliary delivery. These results suggest that newly synthesized PC1 takes distinct pathways to the ciliary and apical membranes. Ciliary PC1 appears to by-pass Brefeldin A sensitive Golgi compartments, while apical delivery of PC1 traverses these compartments.

### Legend for Graphical Abstract:

---

\*\* Address correspondence to: Michael Caplan, Department of Cellular and Molecular Physiology Yale University School of Medicine, P.O. Box 208026, New Haven, CT 06520-8026 Tel: 203-785-7316 michael.caplan@yale.edu.



The polycystin-1 protein undergoes an autocatalytic cleavage that releases its large extracellular N-terminal domain, which remains non-covalently attached to its transmembrane domains. Exposing cells to alkaline pH strips off the N-terminal domain, and this property was employed in an experiment designed to examine the post-synthetic trafficking of polycystin-1. While the apical membrane pool of protein passes through the Golgi complex, the ciliary pool appears to pursue a Golgi-bypass pathway.

### Keywords

ADPKD; PC1; PC2; Rab1A; Golgi bypass; cilia; trafficking

### Introduction

The primary cilium is a specialized organelle that protrudes from the plasma membranes of most sedentary somatic cells. Primary cilia are built around a central cytoskeletal structure composed of a non-motile 9+0 microtubule bundle that is referred to as the ciliary axoneme<sup>1</sup>. In polarized epithelial cells, such as those that line the renal tubule, the primary cilium arises from the apical domain of the plasma membrane. The primary cilium plays roles in mechano- and chemosensation, as well as serving as the functional nexus for multiple signaling pathways. Mutations in proteins found in the primary cilium cause ciliopathies, a class of genetic disorders that are often characterized by the presence of renal cysts and that also manifest additional phenotypes such as neural tube defects, retinal malformations and polydactyly<sup>2</sup>.

Autosomal Dominant Polycystic Kidney Disease (ADPKD) is the most prevalent ciliopathy, affecting approximately one in one thousand individuals. ADPKD causes progressive renal cyst formation, resulting in end-stage renal failure in about half of all ADPKD patients by their sixth decade of life<sup>3</sup>. This disease is caused by pathological mutations in the PKD1 and PKD2 genes, which encode the transmembrane proteins Polycystin-1 and Polycystin-2 (PC1 and PC2), respectively. PC1 is a 450kDa protein with a large extracellular N-terminal domain, 11 predicted membrane-spanning domains, and a 200 amino acid long cytoplasmic C-terminal tail<sup>4,5</sup>. PC1 localizes to desmosomes, adherens junctions, the ciliary membrane, the apical membrane and the lateral domain of epithelial cell plasma membranes<sup>6-10</sup>. Characterized pathogenic mutations in PKD1 can result in the production of decreased

quantities of PC1 protein, or can produce PC1 protein that does not accumulate in at least one of its sites of functional residence<sup>6,10,11</sup>. Little is known, however, regarding the pathways and mechanisms that govern the trafficking of PC1 to each of these membrane domains.

During the course of its post-translational maturation and function an individual PC1 molecule may be modified by one or more cleavages: N-terminal *cis*-autoproteolytic cleavage at the G protein-coupled receptor proteolytic site (GPS) domain located just prior to the first transmembrane domain, and C-terminal cleavages that remove part or all of the cytoplasmic tail<sup>12</sup>. The N-terminal GPS cleavage occurs early in the secretory pathway and the liberated N-terminal domain, which comprises ~3,000 residues, remains non-covalently attached to the membrane-bound ~150 kDa C-terminal fragment (CTF)<sup>12</sup>. The N-terminal cleavage is functionally critical. It appears to be required in order for newly synthesized PC1 to depart the endoplasmic reticulum<sup>13,14</sup>. Mice expressing a mutant form of PC1 that is uncleavable at the N-terminal GPS site do not traffic the PC1 protein appropriately and develop severe renal cysts<sup>15,16</sup>. The C-terminal tail of PC1 contains a nuclear localization sequence (NLS) that targets some of the C-terminal cleavage fragments to the nucleus, where they can participate in modulating the activities of transcription factors<sup>9,17–20</sup>.

PC2 is a nonselective, calcium permeable member of the *tp* family of cation channel with six transmembrane domains. It is most abundantly localized to the endoplasmic reticulum<sup>21,22</sup> and is also expressed in the primary cilium. PC1 and PC2 form a complex that is stabilized by interlocking coiled-coil domains present in each of their intracellular C-termini<sup>23,24</sup>, and they are thought to interact in this fashion in the primary cilium. The PC1 and PC2 complex appears to participate in several processes, including calcium signaling, mechano- and chemosensation, and the modulation of signaling cascades such as the JAK/STAT, AP1 and the Wnt pathways<sup>25</sup>. The interaction between PC1 and PC2 governs aspects of the function and the localization of both proteins<sup>13,16,23,26–29</sup>.

Cilia contain a unique group of resident membrane and soluble proteins, and the delivery of these proteins into the cilium is thought to be a tightly regulated, multi-step process that begins with the docking of cargo-carrying vesicles to elements of the BBSome protein complex at the base of the cilia<sup>30</sup>. Ciliary proteins then travel through a transition zone at the base of the cilium that appears to serve as a selectivity filter that participates in determining which proteins can enter and exit the cilium. Proteins that are permitted to pass through the transition zone subsequently traffic along the ciliary axoneme, which serves as the scaffolding on which the molecular motor-driven intraflagellar transport of selected ciliary proteins takes place<sup>31</sup>.

Proteins that are targeted to the apical plasma membrane are generally believed to be delivered through the classical secretory pathway<sup>32–34</sup>. In the case of apical proteins, this pathway involves sequential, transient residence in the ER and the Golgi complex, after which they may pass through one or more endosomal compartments, including the common or apical endosomes, or apical early endosome, *en route* to the apical plasma membrane<sup>35,36</sup>. An interesting subset of cell surface and ciliary proteins, however, appear to utilize a Golgi-bypass pathway that either completely avoids the Golgi complex or that involves

distinct patterns of residence in or transit through Golgi sub-compartments<sup>32,33,37</sup>. PC2, for example, appears to follow a route to the cilium that includes passage through the cis-Golgi compartment but bypasses the medial and trans-Golgi compartments<sup>37-39</sup>.

Efforts to characterize these non-classical, Golgi-independent protein trafficking pathways often employ Brefeldin-A (BFA), a fungal metabolite that prevents the assembly of the COPI coat complexes necessary for the anterograde trafficking of proteins between the ER and Golgi complex<sup>40</sup>. While BFA treatment blocks anterograde movement of proteins out of the ER, it allows retrograde movement back into the ER, effectively leading to a merger of the cis- and medial Golgi compartments with the ER<sup>41</sup>. BFA treatment also induces the merger of the trans-Golgi compartment with the recycling endosomal system but does not impair the cycling of proteins between the plasma membrane and the endosomes<sup>42</sup>. In addition, protein trafficking through the Golgi complex in mammalian cells can also be blocked by incubating cells at 20°C<sup>43-45</sup>. The mechanism through which this 20°C treatment reversibly blocks Golgi trafficking through the trans-Golgi network remains unelucidated.

Experiments in which polarized epithelial cells were treated with BFA indicate that a growing list of plasma membrane components, including membrane lipids as well as adhesion and signaling proteins, can be trafficked to the cell surface via non-canonical, BFA-insensitive routes<sup>46</sup>. Some of these proteins traverse the Intermediate Compartment (IC), a collection of tubules that are defined by the presence of Rab1 and by resistance to BFA-induced COPI uncoating<sup>34</sup>. The cystic fibrosis transmembrane conductance regulator chloride channel is an example of a protein that appears to bypass at least a portion of the Golgi complex and that manifests transient IC residence, passing through a pericentrosomal subcompartment of the IC on its non-canonical path to the plasma membrane<sup>47</sup>.

The work presented here examines the delivery of PC1 to the apical and ciliary membranes. We have developed a technique that uses immunofluorescence labeling to visualize a temporally defined cohort of PC1 delivered *de novo* to the plasma membrane. We show that the delivery of the apical and ciliary pools of PC1 in the LLC-PK1 line of porcine renal epithelial cells involves two distinct trafficking pathways. Treating cells with BFA inhibits PC1 delivery to the apical but not ciliary membranes. Similarly, incubating cells at 20°C inhibits repopulation of apical PC1, but does not prevent delivery of the ciliary pool of PC1. Finally, we show that a subpopulation of PC1 co-localizes with Rab1a and may, therefore, pass through the BFA-insensitive pericentrosomal recycling compartment within the IC.

## Results

### Alkaline Stripping removes the N-terminus of PC1.

To visualize the trafficking of a temporally defined cohort of PC1, we used LLC-PK1 cells expressing PC1 and PC2. The LLC-PK1 cell line is a useful model in which to study primary cilia trafficking because these cells develop very long cilia, as revealed by immunofluorescence staining using an antibody directed against acetylated tubulin (see Figure 1A) within 5 days following attainment of confluency. To observe the ciliary delivery of PC1 we developed and optimized a protocol that takes advantage of two previously

published observations: first, that the PC1 molecules that reach the plasma membrane in the presence of PC2 are cleaved at the N-terminal GPS site; and second, that the cleaved N-terminal domain of PC1 remains non-covalently attached to the C-terminal membrane-bound portion<sup>12–14,16,28,29,48</sup>. These properties allowed us to identify treatment conditions which, when applied to unfixed, polarized LLC-PK1 cells stably expressing PC1 and PC2 (LLC-PK1 PC1+PC2), resulted in the removal of the Flag-epitope-containing N-terminal fragment of PC1 from the rest of the PC1 protein. We found that treating cells at alkaline pH (pH 9.5) for 45 minutes at 4° C effectively removes the PC1 N-terminus from its non-covalent association with the membrane-bound C-terminus (Figure 1). Labeling with anti-HA antibody to detect the C terminus of the PC1 protein demonstrates that the membrane-associated portion of PC1 is not perturbed by the stripping protocol (Figure 1B). Furthermore, the N terminal fragment that is released by the alkaline stripping procedure can be detected in the media by immunoprecipitation followed by western blotting (Figure S1). Thus, this stripping protocol does not produce its effects on the Flag signal by damaging the membrane or extracting its population of PC1, but instead it causes the non-covalently associated pool of Flag-tagged PC1 N termini to become detached from their C-terminal membrane domains. The anti-Flag immunofluorescence signal from PC1 molecules at the apical plasma membrane was essentially completely removed following strip, while a small signal remained at the base of the primary cilium (Figure 1A and B). This observation suggests either that the stripping of the PC1 N-terminus is less efficient when PC1 is integrated among the densely packed proteins of the cilium or that a small portion of the ciliary pool of PC1 does not undergo cleavage at the GPS site.

### **Surface antibody labeling of cells following strip allows delivery of newly synthesized PC1 to be visualized.**

Because the cells are washed following stripping in order to remove the released PC1 N-termini, reattachment of the eluted N-termini is not possible and hence this protocol for removing the Flag-containing N-terminus is irreversible. Thus, any time-dependent recovery of signal that is detectable by surface immunofluorescence using an anti-Flag antibody must correspond to *de novo* surface expression of PC1 molecules that were not present at the plasma membrane during the stripping protocol. Placing stripped cells back into growth media at 37°C and allowing them to incubate for a sufficient period of time should permit the delivery of new PC1 molecules to the ciliary and plasma membranes, and surface immunofluorescence performed with the anti-Flag antibody after this chase interval should permit the labeling and visualization of the pool of PC1 that is delivered to the cell surface within a defined period of time following the strip. Data from such a “strip-recovery” experiment, in which cells were incubated for 7 hours following the stripping procedure, are presented in Figure 1A and B and quantitated in 1C. An examination of the time course of this recovery is presented in Figures 2A and 2B. Immediately following the stripping procedure, little or no signal is detected with the surface-applied anti-Flag antibody. After 30 minutes of incubation, signal is detectable in the cilia while signal in the apical plasma membrane is not detectable until the one hour time point. Maximal recovery of the ciliary and plasma membrane pool is observed within 6 hours, while recovery of the plasma membrane pool continues for 24 hours. The stripping protocol and the time course of PC1 signal recovery was not cell-type specific, as HEK293 cells expressing PC1 and PC2

exhibited behavior that was similar to that observed with the LLC-PK1 cells (data not shown). Finally, to assess whether the alkaline stripping protocol affects the delivery or recycling of other apical membrane proteins, we used wheat germ agglutinin (WGA) conjugated to two different fluorophores to examine the surface delivery and recycling of a broad cross section of apical membrane proteins. Cells were exposed to the alkaline stripping medium or to control medium, after which they were incubated with WGA-594 to label apical surface glycoproteins. After washing away unbound WGA-594, cells were incubated for 0 minutes or for various time intervals at 37°C and then exposed to WGA-488 to label WGA binding sites that were not blocked by WGA-594 and that thus represent newly-delivered apical glycoproteins. As expected, no WGA-488 labeling was detected after 0 minutes of incubation (Figure S2), whereas after 3 hours there was abundant WGA-488 labeling that was equivalent in both the alkaline stripped sample and the un-stripped control. Furthermore, the signal associated with internalized WGA-594 was the same in both samples. Thus, the alkaline stripping procedure does not appear to perturb the delivery or recycling of a large population of apical membrane proteins.

### **Ciliary delivery of PC1 is BFA insensitive, while apical PC1 delivery is inhibited by BFA treatment.**

The ability to identify readily a temporally defined pool of PC1 molecules following their delivery to the plasma and ciliary membranes provided us with the ability to investigate the trafficking pathways that PC1 takes to these destinations. Cells treated with BFA for 2 hours before being subjected to alkaline stripping and throughout the subsequent recovery period exhibited a restoration of anti-Flag antibody surface immunofluorescence signal at the ciliary membrane, but not at the apical plasma membrane (Figure 3A). At no point during recovery did we find that the appearance of PC1 in the ciliary membrane was preceded by the accumulation of PC1 at the apical membrane. To determine whether the recovery observed in control media as well as the recovery detected in BFA media were attributable to the delivery of newly synthesized protein, we repeated the strip-recovery experiment in the presence or absence of the protein synthesis inhibitor Cycloheximide (CHX). Cells were pretreated with CHX for 2 hours, stripped, and allowed to recover in CHX media (Figure 3B). CHX treatment completely abolished apical recovery, whereas weakly detectable (but not statistically significant) PC1 ciliary recovery was reproducibly observed. This observation suggests the possible existence of a small pre-synthesized pool of PC1 in an intracellular compartment that is able to re-populate specifically the ciliary pool of PC1. It is also possible, however, that because the apical membrane is much larger in surface area compared to the ciliary membrane, a small amount of PC1 recovery to apical membrane under CHX conditions was below the detection threshold of our quantitative analysis. These data are quantitated in Figure 3C. It is important to note that magnitude of the recovery in the ciliary signal that is observed in the presence of BFA is significantly higher than the ciliary recovery that is observed in the presence of CHX. These data indicate that the bulk of the BFA-insensitive ciliary recovery is comprised of newly synthesized PC1.

### **Incubation at 20°C blocks apical delivery of PC1.**

In order to verify that the lack of apical recovery seen in the BFA strip-recovery experiment was attributable to the blocking of protein trafficking through the Golgi complex, we



performed the strip recovery experiment in association with a 20°C block. Incubating cells at 20°C inhibits anterograde protein traffic out of the trans Golgi network<sup>44,45,49</sup>. Cells were pretreated for one hour at 20°C, and allowed to recover post-strip at either 20°C or 37°C. We found that cells that were allowed to recover at 20°C exhibited re-accumulation of PC1-Flag staining in ciliary but not in apical membranes (Figure 4A and B). These data are consistent with those of the BFA experiment and suggest that blocking trafficking through the Golgi complex prevents apical but not ciliary PC1 delivery.

### **The D511V mutant form of PC2 supports ciliary but not apical PC1 trafficking.**

PC1 and PC2 associate with one another and co-localize to the primary cilium<sup>8</sup>, where they are thought to form a heteromeric ion channel complex<sup>23</sup>. To investigate the effect of the channel activity of PC2 on the plasma membrane trafficking of PC1, we performed the strip recovery protocol with an LLC-PK1 cell line expressing WT PC1 as well as PC2-D511V, a naturally occurring pathological mutation of PC2 that lacks ion channel activity<sup>50</sup>. When expressed in association with PC1 in LLC-PK1 cells, the D511V protein is detected in cilia, as has been reported in a previous study<sup>51</sup>. Levels of cytoplasmic PC1 in the PC2-D511V cell line were comparable, as assessed by immunofluorescence, to those in cells expressing WT PC2. While PC1 was detected by surface immunofluorescence in the cilia in the PC2-D511V-expressing cells, no apical PC1 was detectable in these cells (Figure 5A). Though the magnitude of the ciliary PC1 signal is reduced by a factor of 1.9 in PC2-D511V-expressing cells as compared to that detected in their wild type counterparts (Figure 5B), the signal associated with the apical pool of PC1 in these cells is reduced to below our limit of detection. To assess whether the fold reduction in the apical signal in these cells is greater than the fold reduction in the ciliary signal, we examined the data from our strip-recovery experiments to define the quantity of apical signal that is seen in association with each level of ciliary signal throughout the course of the recovery. Signal density in cilia was calculated using Image J by summing the total ciliary area per image and the total cilia-associated fluorescence signal density in the same image. Total ciliary fluorescence signal was then divided by total ciliary area to yield the average fluorescence per pixel of ciliary PC1. We found that the signal density (signal intensity/pixel) at steady state of ciliary PC1 in LLC-PK1 cells expressing PC2-D511V was roughly equivalent to the PC1 signal density observed in cells expressing WT PC2 at 3 hours of recovery post-stripping (91 vs. 94, respectively). The apical PC1 signal at 3 hours of recovery in cells expressing WT PC1 was readily detectable and was significantly different from the signal observed following the strip. Thus, we conclude that the lack of detectable apical PC1 signal in cells expressing PC2-D511V indicates that the apical pool of PC1 is decreased to a much larger extent than is the ciliary pool of this protein. This observation suggests the interesting possibility that PC2's channel activity is required for the apical but not the ciliary delivery of PC1.

### **The PC1 NLS is not required for its ciliary localization.**

Recently, components of the nuclear pore complex have been detected at the base of the primary cilium<sup>52</sup>. It has been suggested that the presence of these nuclear pore proteins at the base of the primary cilium may regulate the delivery of at least some soluble and membrane proteins to the cilium<sup>53</sup>. Other studies indicate that the ciliary population of nuclear pore proteins may not participate directly or structurally in forming the barrier that

controls protein diffusion into the cilium<sup>54,55</sup>. In the case of RP2, a membrane-associated protein that localizes to the cilium, entry of the newly synthesized protein into the ciliary membrane requires the participation of Importin  $\beta$ 2, a component of the nuclear import machinery<sup>56</sup>.

The cytoplasmic C-terminus of PC1 contains an NLS that is necessary to drive the nuclear localization of one of its C-terminal cleavage fragments<sup>9</sup>. We wondered whether this NLS also plays a role in ensuring the ciliary localization of the full length PC1 protein. To test this possibility, we generated a PC1 NLS construct encoding mouse PC1 carrying the N terminal Flag tag and the C terminal HA tag and lacking the 21 amino acid residues that contribute to the C terminal NLS (Leu 4124-Arg 4144). We generated an LLC-PK1 cell line that stably expresses both PC1 NLS and PC2. Analysis by western blotting using an antibody directed against the HA epitope tag revealed that the quantity of the PC1 NLS protein is similar to that observed for the wild type PC1 protein expressed in LLC-PK1 cells. Furthermore, like the wild type PC1 protein, PC1 NLS undergoes cleavage at the GPS site to produce the ~150 kDa CTF (Figure 6A). To assess whether the PC1 NLS protein is targeted to the cilium we performed the anti-Flag surface immunofluorescence protocol. As can be seen in Figure 6B, PC1 NLS is present in cilia, as evidenced by its co-localization with acetylated tubulin. Thus, the NLS present in the C terminus of PC1 is not necessary in order for the PC1 protein to traffic in to the ciliary membrane.

### PC1 colocalizes with Rab1a.

The observation that BFA inhibited the delivery of PC1 to the apical cell surface but had minimal effect on PC1 delivery to the cilium suggested that PC1 does not necessarily require transit through the medial Golgi before reaching the ciliary plasma membrane. The Pericentrosomal Intermediate Compartment plays a role in protein trafficking along the secretory pathway and is also thought to participate in transport that is BFA insensitive<sup>32</sup>. This compartment is organized around the centrosomal centrioles and is notable for the presence of the Rab1a GTPase<sup>34</sup>. Immunofluorescence performed on LLC-PK1-PC1+PC2 cells transfected with GFP-Rab1a revealed partial colocalization between PC1 detected by anti-HA antibody immunofluorescence and the GFP-Rab1a, suggesting that intracellular PC1 accumulates in a Rab1A-positive compartment (Figure 7).

## Discussion

The large size and complex intracellular distribution of the PC1 molecule make it challenging to track PC1's progression through the biosynthetic pathway to the plasma membrane. While immunofluorescence with anti-PC1 antibodies performed on fixed cells can report the protein's steady-state localization, it reveals nothing about the temporal dynamics of the PC1 protein's trafficking. We have developed a novel method that allows us to strip the extracellular, non-covalently bound N-terminal portion of PC1 from its C-terminal transmembrane domain. This allows us to detect the appearance of newly delivered PC1 molecules as they are trafficked to the plasma membrane. In addition, we developed an image analysis method that permitted us to quantify the level of polycystin protein present in the cilium versus at the apical plasma membrane. The results obtained through application



and quantitative analysis of this “strip-recovery” technique provide a unique immunofluorescence-based window into the temporal dynamics of PC1 trafficking. In addition, because the strip-recovery selectively removes the extracellular N-terminal portion of the PC1 proteins while leaving the membrane anchored C-terminal portion of the PC1 protein in place, this technique may be useful in future studies designed to identify those functions of the PC1 protein that are dependent upon the presence of the non-covalently associated N-terminus.

Under control conditions we detected robust post-strip recovery of the PC1 signal at both the apical and ciliary plasma membrane within 5 hours of the strip. When LLC-PK1 cells were incubated with BFA, or when a 20° C temperature block of trafficking out of the trans Golgi network was applied, significant recovery of PC1 signal was only detected at the ciliary membrane. CHX treatment confirmed that the ciliary recovery observed under Golgi block conditions is attributable primarily to the arrival of newly synthesized PC1. In addition, we found that PC1 can traffic to the ciliary membrane in association with a channel defective mutant of PC2, demonstrating that PC2’s channel activity is not required in order to ensure ciliary localization of the complex. In contrast, however, PC2 channel activity may have an effect on PC1’s apical localization, since no apical PC1 was detected when PC1 was expressed in association with a channel defective mutant form of PC2. Finally, we showed that a portion of the intracellular pool of PC1 co-localizes with Rab1a, suggesting that a subset of the cell’s population of PC1 may transit through the Rab1a-positive Intermediate Compartment *en route* to the cilium.

Taken together, these data indicate that the pools of PC1 protein that are bound for the ciliary and the apical membranes are distinct from one another and are differentially sensitive to conditions that impede protein trafficking through the Golgi complex. Our data suggesting that the cilia-targeted subpopulation of PC1 can bypass Golgi compartments *en route* to the ciliary membrane are especially interesting in light of recent observations that indicate that PC2 also pursues distinct routes of delivery to the somatic and ciliary membranes and that it bypasses portions of the Golgi complex as it makes its way to the cilium<sup>37</sup>. Previous experiments have shown that PC2 ciliary trafficking is BFA insensitive but that ciliary PC2 protein exhibits Endo-H insensitivity, suggesting that PC2 traffics through cis-Golgi compartments upon trafficking to the cilium<sup>38,39</sup>. Kim and colleagues have shown that PC1 found in the cilia is Endo-H insensitive, suggesting that at least a portion of PC1 traffics through the cis-Golgi<sup>29</sup>. In addition, at least a portion of newly synthesized PC1 appears to co-localize with markers of the Trans Golgi Network<sup>57</sup> and to assemble with components of the Golgi trafficking machinery<sup>29,57</sup>. However, delivery of both PC1 and PC2 to the cilium appears to be insensitive to inhibition by BFA, suggesting that some or all of the ciliary populations of the PC1 and PC2 proteins may by-pass the trans-Golgi complex during the course of their post-biosynthetic trafficking.

The evidence presented here, showing that PC1 can pursue multiple trafficking routes out of the TGN, is consistent with previous studies that find that the variety of options that are available to proteins *en route* to the cell surface may be more numerous than originally thought. In polarized epithelial cells, for example, multiple distinct vesicular carriers transport basolateral proteins to the basolateral plasma membrane and apical proteins to the

apical surface. Each of these pathways manifests individual characteristics relating to their kinetic properties, inhibitor sensitivities and sites of delivery<sup>58–60</sup>. This multiplicity of pathways available is thus in concert with our observations that pools of PC1 can pursue divergent itineraries with different biochemical properties. The potential role of the PC2 channel activity in the process of the sorting of the PC1-PC2 complex is perhaps surprising and interesting. Previous studies show that the channel-dead D511V mutant form of PC2 supports the maturation and plasma membrane delivery of PC1<sup>13,28</sup>. The effects of the D511V mutant form of PC2 on the differential trafficking of PC1 among the plasma membrane and the cilium has not previously been explored in depth. It is tempting to speculate that the channel activity of PC2 could alter the calcium concentration within the Golgi complex, which has been shown to modulate forward trafficking of secretory proteins<sup>61</sup>. Alternatively, the activity state of the channel may alter its conformation and thus affect its ability to interact with elements of the sorting and trafficking machinery.

Ciliary proteins, including polycystins, are thought to undergo a regulated and specialized process of importation through the ciliary transition zone. To date, several distinct ciliary targeting sequences (CTS) have been identified, including RVxP on the C-terminus of PC2<sup>29,62</sup>. However, little is known about the mechanism through which ciliary proteins are imported into the cilia from the transition zone. A number of studies have suggested that components of the nuclear pore complex and nuclear import machinery may participate in conducting at least some proteins across the ciliary transition zone<sup>52,53,56</sup>. Our data indicate that the NLS that is present in the C terminus of the PC1 is not required in order to target PC1 to the cilium or to allow it to traverse the transition zone.

While both PC1 and PC2 appear to traffic along pathways that are at least partially Golgi-independent, it remains to be determined whether these two proteins are always transported together. Several co-immunoprecipitation studies demonstrate that a portion of PC1 and PC2 populations can exist in a complex with one another<sup>23,28</sup>. It has been suggested that the presence of PC1 allows PC2 to exit the ER and that PC2 enhances the GPS cleavage of PC1<sup>25</sup>. This effect of PC2 expression on PC1 GPS cleavage does not require the stable interaction of PC1 and PC2, suggesting that transient or indirect interactions between PC1 and PC2 may be sufficient to mediate this influence<sup>28</sup>. Recent studies clearly indicate that assembly of PC1 with PC2 and PC1 GPS cleavage are absolute prerequisites for the delivery of PC1 to the cilium<sup>13,16,29</sup>. Future studies that visualize the PC2 protein's appearance at the plasma membrane will be required to reveal whether PC1 and PC2 move in concert through the secretory pathway or pursue independent itineraries through intracellular processing compartments.

As noted above, there is a well-established connection between PC1 cleavage, localization and function. Autocatalytic cleavage at the GPS site appears to be important for establishing appropriate PC1 localization as well as for enabling the physiological function of PC1 *in vivo*<sup>14</sup>. This cleavage, potentiated by co-expression with PC2, is required for the delivery of PC1 to the plasma membrane<sup>19</sup>. The results presented here confirm that the vast majority of PC1 molecules present at the plasma membrane are cleaved at their GPS sites, since essentially all of the PC1 protein at the cell surface is susceptible to the alkaline stripping protocol that separates the products of the GPS cleavage, eluting the N-terminal fragment

from the membrane-associated C-terminal fragment. Both before and after alkaline stripping, we can detect PC1 in the cilium and at the apical plasma membrane using an antibody directed against the HA epitope at the C-terminus of our PC1 construct. These data indicate that a substantial portion of the cell surface population of PC1 has not undergone any C-terminal cleavages (Fig. 1B). These C-terminal cleavages release soluble fragments of the PC1 cytoplasmic C terminal tail that translocate to the nucleus and interact with transcription factors to modify gene transcription<sup>18,20,63</sup>. These cleavages may be affected by extracellular stimuli, since abrogating flow through a kidney increases the release and nuclear localization of these C-terminal fragments<sup>9,63</sup>. Our data suggest that stripping the extracellular N terminal domain away from the membrane resident C-terminal fragment of PC1 does not trigger a substantial increase in the extent of C-terminal tail cleavage.

Our results demonstrating the recovery of the ciliary PC1 signal after 30 minutes are consistent with imaging studies performed on other ciliary proteins, which have shown that delivery of newly synthesized protein to the cilia can be detected within one hour. One such protein is Smoothed, a G-protein coupled receptor that traffics via Golgi bypass to the somatic plasma membrane and eventually to the ciliary membrane<sup>64</sup>. Similarly, the newly synthesized Autosomal Recessive Polycystic Kidney Disease ciliary protein fibrocystin can be detected in cilia as early as 30 minutes, and reaches steady state levels within two to four hours. Fibrocystin seems to target directly to cilia without integrating into the somatic plasma membrane<sup>65</sup>, however it is unknown whether the trafficking of fibrocystin is BFA insensitive and therefore likely to involve a route that bypasses the Golgi. Apical PC1 recovery took significantly longer than ciliary PC1 recovery, with significant apical staining detected only after 3 hours. One possibility for this discrepancy is that if equal amounts of PC1 are being delivered to the ciliary and apical membranes, the fluorescence signal of apical PC1 would be lower because of the large surface area of the apical membrane compared to the ciliary membrane. Further studies are needed to investigate if the time difference in apical and ciliary PC1 trafficking may reflect the limitations of our quantification method or if this difference reflects a real difference in trafficking time between apical and ciliary PC1.

Since it was identified over fifteen years ago, the PC1 protein has only reluctantly revealed the details of its functions and of the factors that influence them. The work presented here demonstrates that PC1 travels to the ciliary membrane through a non-canonical BFA-independent trafficking route that may involve passage through the Intermediate Compartment. These observations have been made possible by the development of a tool that permits the kinetic behavior of temporally defined cohorts of PC1 to be directly visualized. Future application of this technique should make it possible to further characterize the behaviors of specific subpopulations of PC1 and to develop a more complete understanding of how PC1 is regulated as it moves through the secretory pathway.

## Materials and Methods:

### Cell culture and transfections

LLC-PK1 cells were grown at 37°C in alpha-MEM (Invitrogen, Carlsbad, CA) supplemented with 10% FBS, 1% penicillin/streptomycin and 1% L-glutamine. LLC-PK1

cells stably expressing PC1 and PC2 (LL-CPK1 1+2) and LLC-PK1 cells stably expressing WT PC1 and PC2-D511V (LL-CPK1 1+2-D511V) were created by transfection employing Lipofectamine (Invitrogen) according to the manufacturer's instructions. The cDNA plasmids encoding N-terminally FLAG tagged and C-terminally HA-tagged mouse PC1, C-terminally Myc-tagged mouse PC2 and C-terminally Myc-tagged PC2-D511V have been previously described<sup>22</sup>. The cDNA plasmid encoding N-terminally FLAG tagged and C-terminally HA-tagged mouse PC1 NLS was generated by deletion of the base pairs corresponding to amino acids Leu4124-Arg4144 from the plasmid encoding the full-length wild type PC1. Selection for PC1 expression was performed with 1mg/ml G418 (Gibco), while selection for stable PC2 expression was performed using 200mg/ml Zeocin (Invitrogen). To generate LLC-PK1 cells stably expressing GFP-tagged Rab1A, selection was performed using Hygromycin B (Invitrogen). The sequence encoding full-length canine Rab1A was cloned behind the sequence encoding eGFP<sup>47</sup>. The eGFP tag and Rab1A sequence were moved together into a pcDNA3.1 hygromycin-resistant plasmid (Invitrogen) by subcloning at NheI and BamHI sites.

### Antibodies

PC1 was detected using a polyclonal rabbit anti-FLAG antibody (Sigma-Aldrich) that recognizes the N-terminal epitope tag, or a monoclonal mouse anti-HA antibody (Covance, Princeton, NJ) that recognizes the C-terminal epitope tag. Polycystin-2 was detected using anti-c-Myc antibodies (monoclonal from Santa Cruz Biotechnology, Santa Cruz, CA). Cilia were marked using a monoclonal anti-acetylated tubulin antibody (clone 6-11B-1, Sigma-Aldrich). Goat anti-mouse and anti-rabbit IgG secondary antibodies were conjugated to Alexa Fluor 594 and 488 dyes (Invitrogen), respectively. All antibody dilutions for immunofluorescence were 1:500.

### Surface immunofluorescence

LLC-PK1 cells were plated on Transwell polycarbonate filters (Corning Life Sciences) at 150,000 cells/ml and then allowed to grow to and past confluency for a total of five days. To stain the surface population of the PC1 protein, the cells were incubated for one hour in a humidified chamber at 4°C with polyclonal anti-Flag antibody diluted in a blocking buffer of 0.1% BSA in PBS<sup>++</sup> (PBS with 100 μM CaCl<sub>2</sub> and 1 mM MgCl). Cells were then washed with cold PBS<sup>++</sup>, fixed for 20 minutes in 4% paraformaldehyde, permeabilized in PBS<sup>++</sup> with 0.3% TritonX-100 and 0.1% BSA, and blocked for 30 minutes in goat serum dilution buffer (GSDB; 16% goat serum, 400 mM sodium phosphate, 0.3% Triton X-100, and 450 mM NaCl). Fixed cells were incubated in a humidified chamber at room temperature with monoclonal anti-HA primary antibody diluted in GSDB for one hour. Cells were washed with PBS<sup>++</sup> and permeabilized a second time in 0.3% TritonX-100 and 0.1% BSA. Cells were then incubated for one hour with the Alexa Fluor-conjugated secondary antibodies diluted in GSDB. Subsequently, cells were treated with 1:10,000 dilution of Hoechst dye to stain nuclei before mounting. For a more detailed description of this method, see Chapin *et al.*, 2009 and 2010<sup>28,66</sup>.

## Stripping and recovery

To strip the cleaved extracellular and non-covalently attached N-terminus of PC1 from cells, a confluent LLC-PK1 1+2 cell monolayer was washed once in cold (4°C) blocking buffer (0.1% BSA in PBS<sup>++</sup>) and then incubated for 45 minutes at 4°C in alpha-MEM with pH adjusted to 9.5 (stripping buffer). Cells were then rinsed once with cold blocking buffer, once with warm media, and then incubated at 37°C in warm media, supplemented with compounds as specified, for the indicated times. After the recovery period the cells were treated according to the surface immunofluorescence protocol as described above. Three control conditions were used for each strip experiment: “control” cells were washed once with cold blocking buffer and then incubated with the anti-Flag antibody for surface immunofluorescence without being exposed to any stripping buffer. “Stripped” cells were incubated with the stripping buffer for 45 minutes, and subsequently washed with cold blocking buffer before being put directly into an incubation with anti-Flag antibody for the surface immunofluorescence protocol, without any recovery incubation in 37°C medium. “Strip-recovery” cells were subjected to the stripping protocol and subsequently incubated at 37° C for various intervals prior to antibody labeling. Drug treated cells were incubated in 150 µg/ml cyclohexamide or 10 µg/ml Brefeldin-A (Sigma-Aldrich) at 37° C for the indicated times. Cells were incubated with drugs for 2 hours pre-strip, and maintained in “recovery” incubations for up to 7 hours post-strip before undergoing the surface immunofluorescence protocol.

## Image acquisition and quantification

Images were obtained with a Zeiss LSM780 confocal microscope. Unless otherwise noted all images, including those used for quantification, are vertical z-stack compressions of cell monolayers so as to include both the cilium and the cell surface. For quantification, Image J (National Institutes of Health, Bethesda, MD) was used to threshold images identically across conditions and then calculate a fluoresce intensity. Image acquisition settings were chosen to ensure that all pixels were within the linear range. The same settings were applied to analyze the samples from all of the experimental conditions employed in each experiment. Thresholds were chosen based on the level of signal obtained with untransfected cells. Thus, issues of saturation and thresholding should not affect the quantitative analysis of the data. For image quantification, fluorescent immunostaining for acetylated tubulin was used in combination with an ImageJ ROI importer plugin to calculate the irregular outline coordinates of the cilia. This outline was then imposed onto the anti-Flag image that reported the distribution of the extracellular PC1 N-terminus and the mean fluorescence intensity of each cilium within these outlines was calculated. The quantitative data for each condition represent the mean of the pixel densities obtained for 300 cilia. The intensity of apical PC1 staining was determined by calculating the absolute intensity of the PC1-FLAG surface fluorescence for each Z-stack image and subtracting the absolute value of the fluorescence intensity of the corresponding cilium within the z-stack. Apical PC1 values represent an average of 3 z-stack image composites per condition. All statistical comparisons were performed using the unpaired Student's t-test (two-tailed).

## Supplementary Material

Refer to Web version on PubMed Central for supplementary material.

### Acknowledgements:

The authors are grateful to Dr. Jaakko Saraste and to all of the members of the Caplan laboratory for helpful discussions and suggestions. This work was supported by Department of Defense Peer Reviewed Medical Research Program grant number W81XWH-10-1-0504 (MJC), NIH P30 DK090744 (MJC), NIH training grant 5T32GM007223-35 (ALG and HCC) and NSF Graduate Research Fellowship 2005019941 (HCC).

### Abbreviations:

<b>PC1</b>	Polycystin 1
<b>PC2</b>	Polycystin 2
<b>IF</b>	immunofluorescence
<b>ADPKD</b>	Autosomal Dominant Polycystic Kidney Disease
<b>IC</b>	Intermediate Compartment
<b>BFA</b>	Brefeldin A
<b>CHX</b>	Cycloheximide

### References:

1. Singla V, Reiter JF. The primary cilium as the cell's antenna: signaling at a sensory organelle. *Science*. 2006;313(5787):629–633. [PubMed: 16888132]
2. Badano JL, Mitsuma N, Beales PL, Katsanis N. The ciliopathies: an emerging class of human genetic disorders. *Annual review of genomics and human genetics*. 2006;7:125–148.
3. Gabow PA. Autosomal dominant polycystic kidney disease. *N Engl J Med*. 1993;329(5):332–342. [PubMed: 8321262]
4. Nims N, Vassmer D, Maser RL. Transmembrane domain analysis of polycystin-1, the product of the polycystic kidney disease-1 (PKD1) gene: evidence for 11 membrane-spanning domains. *Biochemistry*. 2003;42(44):13035–13048. [PubMed: 14596619]
5. Roitbak T, Surviladze Z, Tikkanen R, Wandinger-Ness A. A polycystin multiprotein complex constitutes a cholesterol-containing signalling microdomain in human kidney epithelia. *Biochem J*. 2005;392(Pt 1):29–38. [PubMed: 16038619]
6. Hughes J, Ward CJ, Peral B, et al. The polycystic kidney disease 1 (PKD1) gene encodes a novel protein with multiple cell recognition domains. *Nat Genet*. 1995;10(2):151–160. [PubMed: 7663510]
7. Boletta A, Qian F, Onuchic LF, et al. Biochemical characterization of bona fide polycystin-1 in vitro and in vivo. *Am J Kidney Dis*. 2001;38(6):1421–1429. [PubMed: 11728985]
8. Yoder BK, Hou X, Guay-Woodford LM. The polycystic kidney disease proteins, polycystin-1, polycystin-2, polaris, and cystin, are co-localized in renal cilia. *J Am Soc Nephrol*. 2002;13(10):2508–2516. [PubMed: 12239239]
9. Chauvet V, Tian X, Husson H, et al. Mechanical stimuli induce cleavage and nuclear translocation of the polycystin-1 C terminus. *J Clin Invest*. 2004;114(10):1433–1443. [PubMed: 15545994]
10. Russo RJ, Husson H, Joly D, et al. Impaired formation of desmosomal junctions in ADPKD epithelia. *Histochemistry and cell biology*. 2005;124(6):487–497. [PubMed: 16187067]



11. Takiar V, Caplan MJ. Polycystic kidney disease: Pathogenesis and potential therapies. *Biochim Biophys Acta*. 2010.
12. Wei W, Hackmann K, Xu H, Germino G, Qian F. Characterization of cis-autoproteolysis of polycystin-1, the product of human polycystic kidney disease 1 gene. *J Biol Chem*. 2007;282(30):21729–21737. [PubMed: 17525154]
13. Gainullin VG, Hopp K, Ward CJ, Hommerding CJ, Harris PC. Polycystin-1 maturation requires polycystin-2 in a dose-dependent manner. *J Clin Invest*. 2015;125(2):607–620. [PubMed: 25574838]
14. Kurbegovic A, Kim H, Xu H, et al. Novel functional complexity of polycystin-1 by GPS cleavage in vivo: role in polycystic kidney disease. *Mol Cell Biol*. 2014;34(17):3341–3353. [PubMed: 24958103]
15. Yu S, Hackmann K, Gao J, et al. Essential role of cleavage of Polycystin-1 at G protein-coupled receptor proteolytic site for kidney tubular structure. *Proc Natl Acad Sci U S A*. 2007;104(47):18688–18693. [PubMed: 18003909]
16. Cai Y, Fedeles SV, Dong K, et al. Altered trafficking and stability of polycystins underlie polycystic kidney disease. *J Clin Invest*. 2014.
17. Lal M, Song X, Pluznick J, et al. Polycystin-1 C-terminal tail associates with beta-catenin and inhibits canonical Wnt signaling. *Hum Mol Genet*. 2008;17(20):3105–3117. [PubMed: 18632682]
18. Merrick D, Chapin H, Baggs JE, et al. The gamma-Secretase Cleavage Product of Polycystin-1 Regulates TCF and CHOP-Mediated Transcriptional Activation through a p300-Dependent Mechanism. *Dev Cell*. 2012;22(1):197–210. [PubMed: 22178500]
19. Bertuccio CA, Chapin HC, Cai Y, et al. Polycystin-1 C-terminal cleavage is modulated by polycystin-2 expression. *J Biol Chem*. 2009;284(31):21011–21026. [PubMed: 19491093]
20. Talbot JJ, Shillingford JM, Vasanth S, et al. Polycystin-1 regulates STAT activity by a dual mechanism. *Proc Natl Acad Sci U S A*. 2011;108(19):7985–7990. [PubMed: 21518865]
21. Cai Y, Maeda Y, Cedzich A, et al. Identification and characterization of polycystin-2, the PKD2 gene product. *J Biol Chem*. 1999;274(40):28557–28565. [PubMed: 10497221]
22. Grimm DH, Cai Y, Chauvet V, et al. Polycystin-1 distribution is modulated by polycystin-2 expression in mammalian cells. *J Biol Chem*. 2003;278(38):36786–36793. [PubMed: 12840011]
23. Hanaoka K, Qian F, Boletta A, et al. Co-assembly of polycystin-1 and -2 produces unique cation-permeable currents. *Nature*. 2000;408(6815):990–994. [PubMed: 11140688]
24. Newby LJ, Streets AJ, Zhao Y, Harris PC, Ward CJ, Ong AC. Identification, characterization, and localization of a novel kidney polycystin-1-polycystin-2 complex. *J Biol Chem*. 2002;277(23):20763–20773. [PubMed: 11901144]
25. Chapin HC, Caplan MJ. The cell biology of polycystic kidney disease. *J Cell Biol*. 2010;191(4):701–710. [PubMed: 21079243]
26. Nauli SM, Alenghat FJ, Luo Y, et al. Polycystins 1 and 2 mediate mechanosensation in the primary cilium of kidney cells. *Nat Genet*. 2003;33(2):129–137. [PubMed: 12514735]
27. Babich V, Zeng WZ, Yeh BI, et al. The N-terminal extracellular domain is required for polycystin-1-dependent channel activity. *J Biol Chem*. 2004;279(24):25582–25589. [PubMed: 15060061]
28. Chapin HC, Rajendran V, Caplan MJ. Polycystin-1 Surface Localization Is Stimulated by Polycystin-2 and Cleavage at the G Protein-coupled Receptor Proteolytic Site. *Mol Biol Cell*. 2010;21(24):4338–4348. [PubMed: 20980620]
29. Kim H, Xu H, Yao Q, et al. Ciliary membrane proteins traffic through the Golgi via a Rabep1/GGA1/Arl3-dependent mechanism. *Nature communications*. 2014;5:5482.
30. Jin H, White SR, Shida T, et al. The conserved Bardet-Biedl syndrome proteins assemble a coat that traffics membrane proteins to cilia. *Cell*. 2010;141(7):1208–1219. [PubMed: 20603001]
31. Pedersen LB, Rosenbaum JL. Intraflagellar transport (IFT) role in ciliary assembly, resorption and signalling. *Current topics in developmental biology*. 2008;85:23–61. [PubMed: 19147001]
32. Marie M, Sannerud R, Avsnes Dale H, Saraste J. Take the ‘A’ train: on fast tracks to the cell surface. *Cell Mol Life Sci*. 2008;65(18):2859–2874. [PubMed: 18726174]

33. Hsiao YC, Tuz K, Ferland RJ. Trafficking in and to the primary cilium. *Cilia*. 2012;1(1):4. [PubMed: 23351793]
34. Marie M, Dale HA, Sannerud R, Saraste J. The function of the intermediate compartment in pre-Golgi trafficking involves its stable connection with the centrosome. *Mol Biol Cell*. 2009;20(20):4458–4470. [PubMed: 19710425]
35. Nickel W, Seedorf M. Unconventional mechanisms of protein transport to the cell surface of eukaryotic cells. *Annual review of cell and developmental biology*. 2008;24:287–308.
36. Stoops EH, Caplan MJ. Trafficking to the apical and basolateral membranes in polarized epithelial cells. *J Am Soc Nephrol*. 2014;25(7):1375–1386. [PubMed: 24652803]
37. Hoffmeister H, Babinger K, Gurster S, et al. Polycystin-2 takes different routes to the somatic and ciliary plasma membrane. *J Cell Biol*. 2011;192(4):631–645. [PubMed: 21321097]
38. Kottgen M, Walz G. Subcellular localization and trafficking of polycystins. *Pflugers Arch*. Vol 451 2005:286–293.
39. Kottgen M, Benzing T, Simmen T, et al. Trafficking of TRPP2 by PACS proteins represents a novel mechanism of ion channel regulation. *Embo J*. 2005;24(4):705–716. [PubMed: 15692563]
40. Donaldson JG, Finazzi D, Klausner RD. Brefeldin A inhibits Golgi membrane-catalysed exchange of guanine nucleotide onto ARF protein. *Nature*. 1992;360(6402):350–352. [PubMed: 1448151]
41. Lippincott-Schwartz J, Yuan L, Tipper C, Amherdt M, Orci L, Klausner RD. Brefeldin A's effects on endosomes, lysosomes, and the TGN suggest a general mechanism for regulating organelle structure and membrane traffic. *Cell*. 1991;67(3):601–616. [PubMed: 1682055]
42. Stephens RE. Ciliary protein turnover continues in the presence of inhibitors of golgi function: evidence for membrane protein pools and unconventional intracellular membrane dynamics. *J Exp Zool*. 2001;289(6):335–349. [PubMed: 11351321]
43. Saraste J, Kuismanen E. Pre- and post-Golgi vacuoles operate in the transport of Semliki Forest virus membrane glycoproteins to the cell surface. *Cell*. 1984;38(2):535–549. [PubMed: 6432345]
44. Matlin KS, Simons K. Reduced temperature prevents transfer of a membrane glycoprotein to the cell surface but does not prevent terminal glycosylation. *Cell*. 1983;34(1):233–243. [PubMed: 6883510]
45. Griffiths G, Pfeiffer S, Simons K, Matlin K. Exit of newly synthesized membrane proteins from the trans cisterna of the Golgi complex to the plasma membrane. *J Cell Biol*. 1985;101(3):949–964. [PubMed: 2863275]
46. Grieve AG, Rabouille C. Golgi bypass: skirting around the heart of classical secretion. *Cold Spring Harbor perspectives in biology*. 2011;3(4).
47. Sannerud R, Marie M, Nizak C, et al. Rab1 defines a novel pathway connecting the pre-Golgi intermediate compartment with the cell periphery. *Mol Biol Cell*. 2006;17(4):1514–1526. [PubMed: 16421253]
48. Qian F, Boletta A, Bhunia AK, et al. Cleavage of polycystin-1 requires the receptor for egg jelly domain and is disrupted by human autosomal-dominant polycystic kidney disease 1-associated mutations. *Proc Natl Acad Sci U S A*. 2002;99(26):16981–16986. [PubMed: 12482949]
49. Saraste J, Palade GE, Farquhar MG. Temperature-sensitive steps in the transport of secretory proteins through the Golgi complex in exocrine pancreatic cells. *Proc Natl Acad Sci U S A*. 1986;83(17):6425–6429. [PubMed: 3462704]
50. Koulen P, Cai Y, Geng L, et al. Polycystin-2 is an intracellular calcium release channel. *Nat Cell Biol*. 2002;4(3):191–197. [PubMed: 11854751]
51. Choi YH, Suzuki A, Hajarnis S, et al. Polycystin-2 and phosphodiesterase 4C are components of a ciliary A-kinase anchoring protein complex that is disrupted in cystic kidney diseases. *Proc Natl Acad Sci U S A*. 2011;108(26):10679–10684. [PubMed: 21670265]
52. Kee HL, Dishinger JF, Blasius TL, Liu CJ, Margolis B, Verhey KJ. A size-exclusion permeability barrier and nucleoporins characterize a ciliary pore complex that regulates transport into cilia. *Nat Cell Biol*. 2012;14(4):431–437. [PubMed: 22388888]
53. Kee HL, Verhey KJ. Molecular connections between nuclear and ciliary import processes. *Cilia*. 2013;2(1):11. [PubMed: 23985042]

54. Breslow DK, Koslover EF, Seydel F, Spakowitz AJ, Nachury MV. An in vitro assay for entry into cilia reveals unique properties of the soluble diffusion barrier. *J Cell Biol.* 2013;203(1):129–147. [PubMed: 24100294]
55. Del Viso F, Huang F, Myers J, et al. Congenital Heart Disease Genetics Uncovers Context-Dependent Organization and Function of Nucleoporins at Cilia. *Dev Cell.* 2016;38(5):478–492. [PubMed: 27593162]
56. Hurd TW, Fan S, Margolis BL. Localization of retinitis pigmentosa 2 to cilia is regulated by Importin beta2. *J Cell Sci.* 2011;124(Pt 5):718–726. [PubMed: 21285245]
57. Ward HH, Brown-Glaberman U, Wang J, et al. A conserved signal and GTPase complex are required for the ciliary transport of polycystin-1. *Mol Biol Cell.* 2011;22(18):3289–3305. [PubMed: 21775626]
58. Farr GA, Hull M, Mellman I, Caplan MJ. Membrane proteins follow multiple pathways to the basolateral cell surface in polarized epithelial cells. *J Cell Biol.* 2009;186(2):269–282. [PubMed: 19620635]
59. Farr GA, Hull M, Stoops EH, Bateson R, Caplan MJ. Dual pulse-chase microscopy reveals early divergence in the biosynthetic trafficking of the Na,K-ATPase and E-cadherin. *Mol Biol Cell.* 2015;26(24):4401–4411. [PubMed: 26424804]
60. Stoops EH, Hull M, Olesen C, et al. The periciliary ring in polarized epithelial cells is a hot spot for delivery of the apical protein gp135. *J Cell Biol.* 2015;211(2):287–294. [PubMed: 26504168]
61. Crevenna AH, Blank B, Maiser A, et al. Secretory cargo sorting by Ca<sup>2+</sup>-dependent Cab45 oligomerization at the trans-Golgi network. *J Cell Biol.* 2016;213(3):305–314. [PubMed: 27138253]
62. Follit JA, Li L, Vucica Y, Pazour GJ. The cytoplasmic tail of fibrocystin contains a ciliary targeting sequence. *J Cell Biol.* 2010;188(1):21–28. [PubMed: 20048263]
63. Low SH, Vasanth S, Larson CH, et al. Polycystin-1, STAT6, and P100 function in a pathway that transduces ciliary mechanosensation and is activated in polycystic kidney disease. *Dev Cell.* 2006;10(1):57–69. [PubMed: 16399078]
64. Milenkovic L, Scott MP, Rohatgi R. Lateral transport of Smoothened from the plasma membrane to the membrane of the cilium. *Journal of Cell Biology.* 2009;187(3):365–374. [PubMed: 19948480]
65. Follit JA, Pazour GJ. Analysis of ciliary membrane protein dynamics using SNAP technology. *Methods Enzymol.* 2013;524:195–204. [PubMed: 23498741]
66. Chapin HC, Rajendran V, Capasso A, Caplan MJ. Detecting the surface localization and cytoplasmic cleavage of membrane-bound proteins. *Methods Cell Biol.* 2009;94:223–239. [PubMed: 20362093]

**Synopsis:**

Polycystin-1 is a large membrane protein that traffics to the primary cilium and the apical surface in polarized LLC-PK1 renal epithelial cells. Polycystin-1 undergoes a cleavage, producing an N-terminal fragment that remains non-covalently associated with the membrane-spanning C-terminal fragment. Exposing cells to alkaline pH disrupts association and removes the N-terminal fragment. We exploit this behavior to perform synchronization studies, revealing that at least some portion of newly synthesized polycystin-1 travels to the cilium via a Golgi bypass pathway.

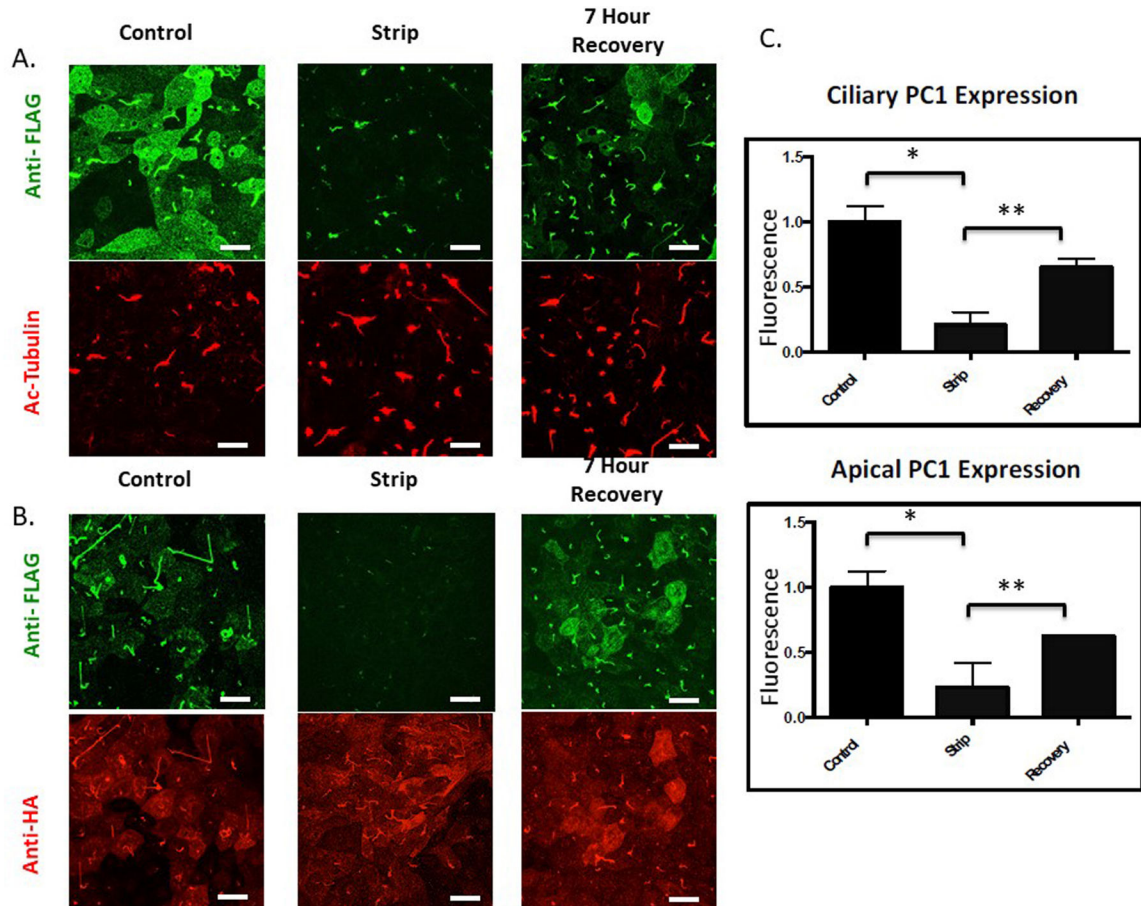


**Figure 1: The extracellular N-terminal fragment of PC1 can be removed by alkaline stripping from the transmembrane portion of the protein.**

**A** Surface expression of PC1 was detected at the apical and ciliary membranes of LLC-PK1 cells stably expressing both PC1 and PC2 through application of a surface immunofluorescence protocol utilizing an anti-Flag antibody to detect the extracellular Flag epitope on the N-terminus of PC1. LLC-PK1 cells stably expressing PC1 and PC2 were “stripped” for 45 minutes at 4°C in a buffered solution with a pH of 9.5 to remove the Flag-tagged N-terminus. Incubation with stripping buffer caused a dramatic decrease in the amount of protein detected by the extracellular application of the anti-Flag. When cells were allowed to incubate for 7 hours after the stripping procedure, the extracellular Flag signal recovered at both the ciliary and apical membranes (upper panels). Fixed and permeabilized cells were incubated with an antibody directed against acetylated tubulin to visualize cilia morphology and length, which were not affected by incubation in an alkaline solution. (lower panels) **B** PC1 was detected using an antibody directed against the HA epitope at PC1’s intracellular C-terminal tail (lower panel). The alkaline stripping protocol did not decrease the magnitude or distribution of the signal associated with the PC1 C terminus. **C** Quantitation of PC1 N-terminus surface expression as a function of strip conditions. Extracellular Flag staining for apical and ciliary PC1 is significantly reduced following strip at pH 9.5 and exhibits a significant recovery following incubation for 7 hours in control

media. (Apical panel: \*  $p < 0.04$ ; \*\*  $p < 0.0034$ ; Cilia panel: \*  $p < 0.025$ ; \*\*  $p < 0.013$ ) All scale bars correspond to 25  $\mu$ . N=3

Author Manuscript

Author Manuscript

Author Manuscript

Author Manuscript



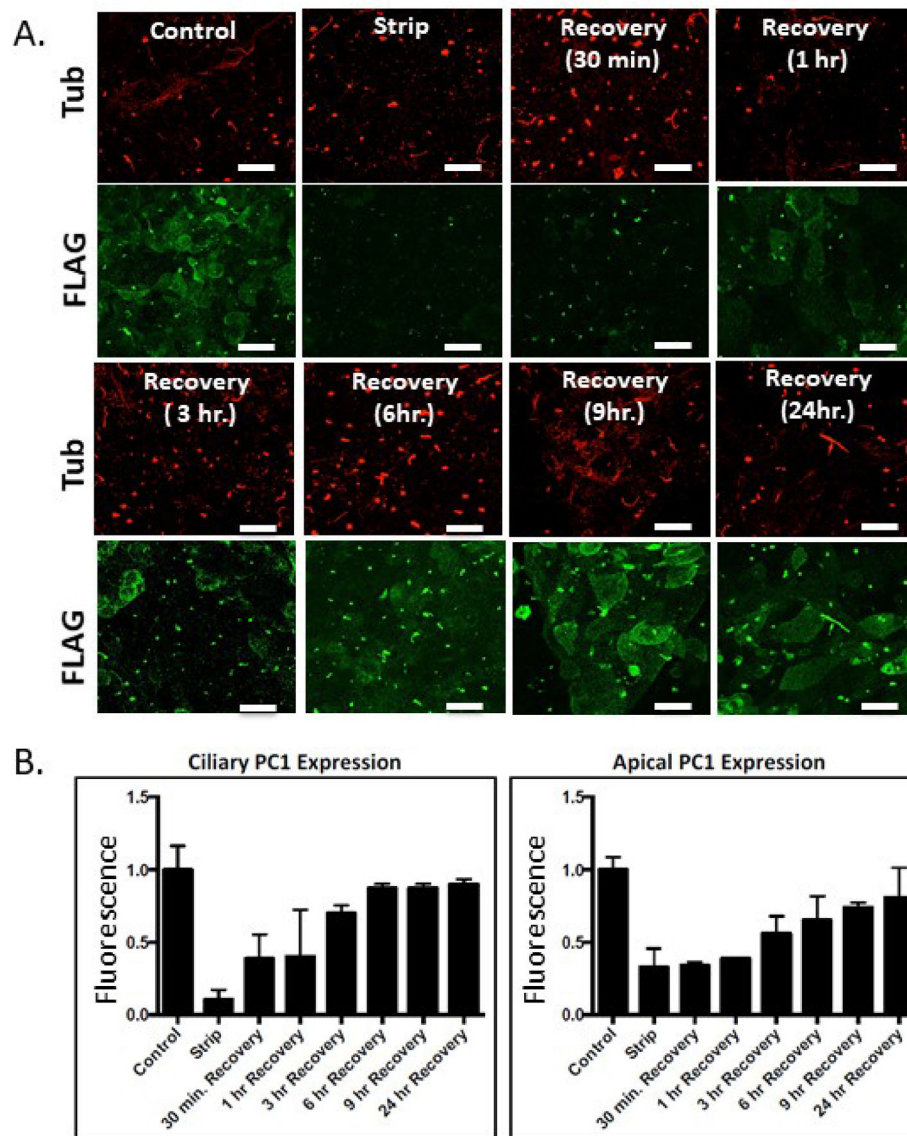


**Figure 2: Time course of recovery of surface PC1 signal following alkaline stripping**

**A** Alkaline stripping was performed followed by recovery incubations of 30 min, 1 hr, 3 hr, 6 hr, 9 hr, 24 hr. Newly delivered ciliary PC1 can be seen within 30 minutes after removal of the N-terminus, while significant apical recovery is detected at 3 hours. **B** Quantitation of data from experiments following the design depicted in **A**. Error bars represent the SEM. All scale bars correspond to 25  $\mu$ . N=3

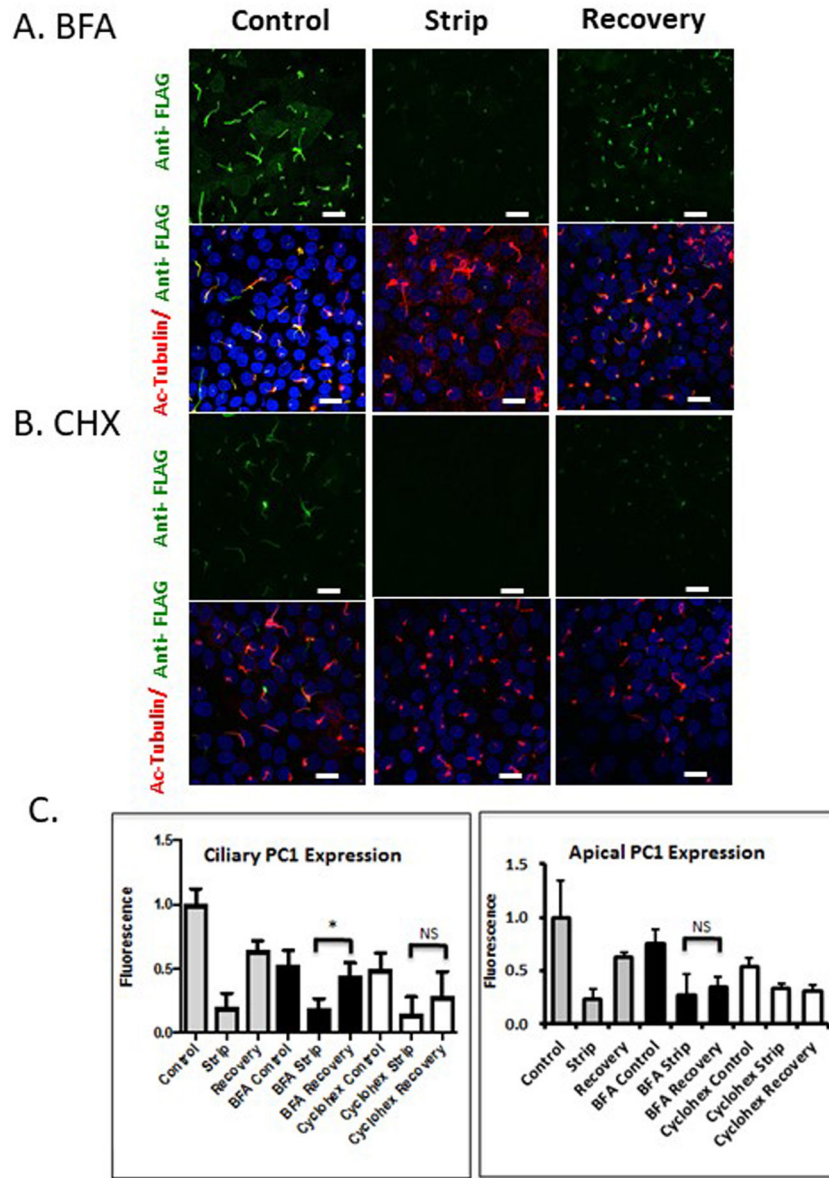


**Figure 3: BFA treatment inhibits PC1 delivery to the apical plasma membrane but not to the cilium.**

**A and B** LLC-PK1 cells stably expressing PC1 and PC2 were subjected to the alkaline stripping protocol to remove the Flag-tagged PC1 N-terminus, and then allowed to recover for 7 hours. Cells treated with BFA (**A**) or CHX (**B**) received drug treatment for 2 hours preceding strip, and during the 7 hours of recovery. Anti-Flag antibody staining is presented in a z-stack of confocal images counter-stained with anti-acetylated tubulin to identify the cilia. **C** Quantification of average pixel intensity of n=300 cilia (left panel) shows ciliary recovery in control conditions and cells treated with BFA. Significant apical recovery (right panel, \* p<0.05) was detected under control conditions, but not in cells treated with BFA. No significant apical recovery was detected in CHX treated cells, but modest ciliary recovery persisted. All scale bars correspond to 25 μ. N=3

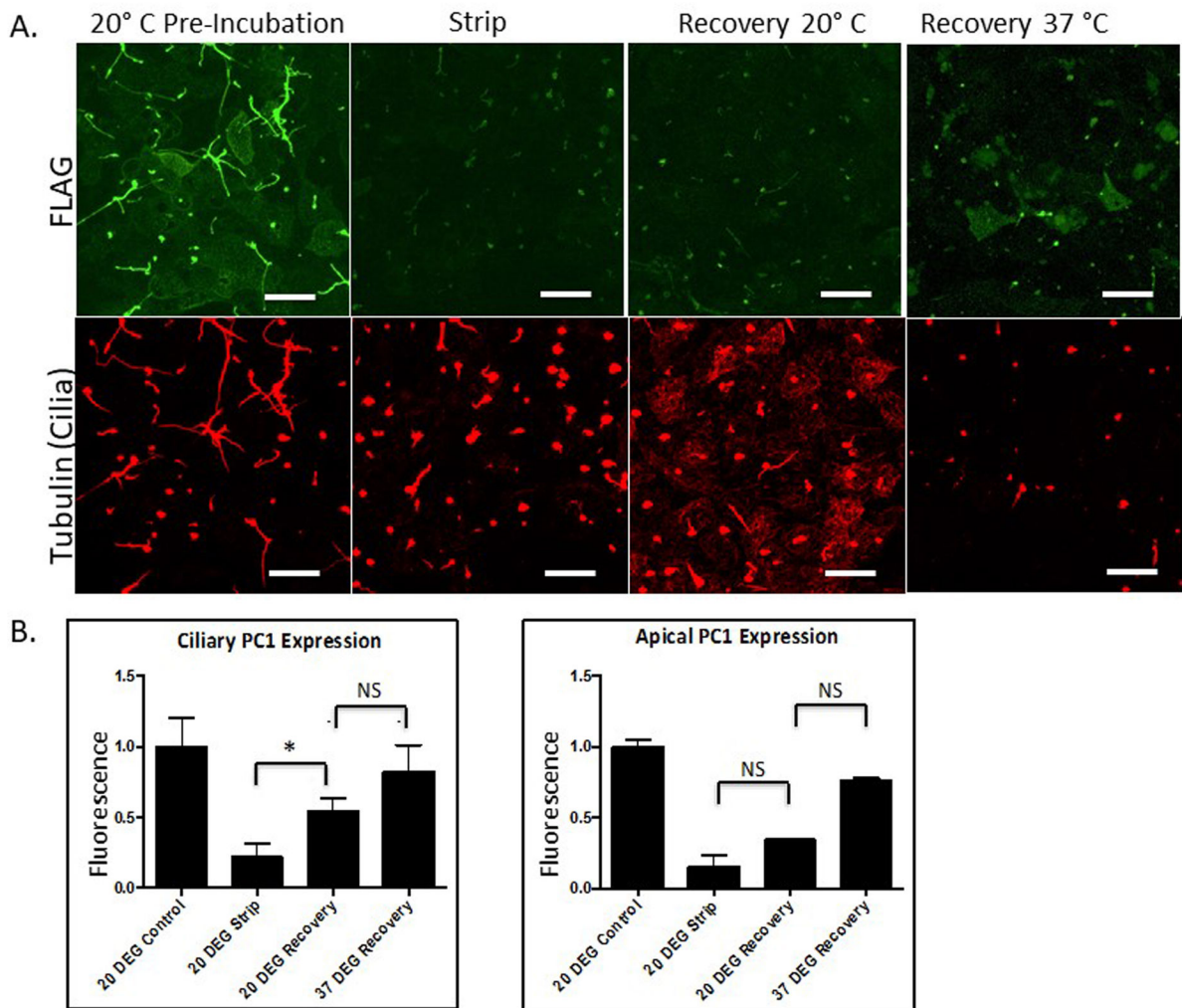


**Figure 4: Incubating cells at 20°C substantially slows apical PC1 recovery but does not prevent ciliary recovery.**

Strip-Recovery was performed on LLC-PK1 cells expressing PC1 and PC2. Cells were incubated at 20° C for 1 hour before incubation in the alkaline stripping buffer. Post strip, cells were incubated at either 20°C or 37 °C. **A** Surface expression of PC1 was detected under the different conditions by surface immunofluorescence utilizing an anti-Flag antibody to detect the extracellular Flag epitope on the N-terminus of PC1. Cilia were detected using an antibody directed against acetylated tubulin. **B** Quantitation of data from experiments following the design depicted in **A**. Error bars represent the SEM. (\*  $p < 0.013$ ) All scale bars correspond to 25  $\mu$ . N=3

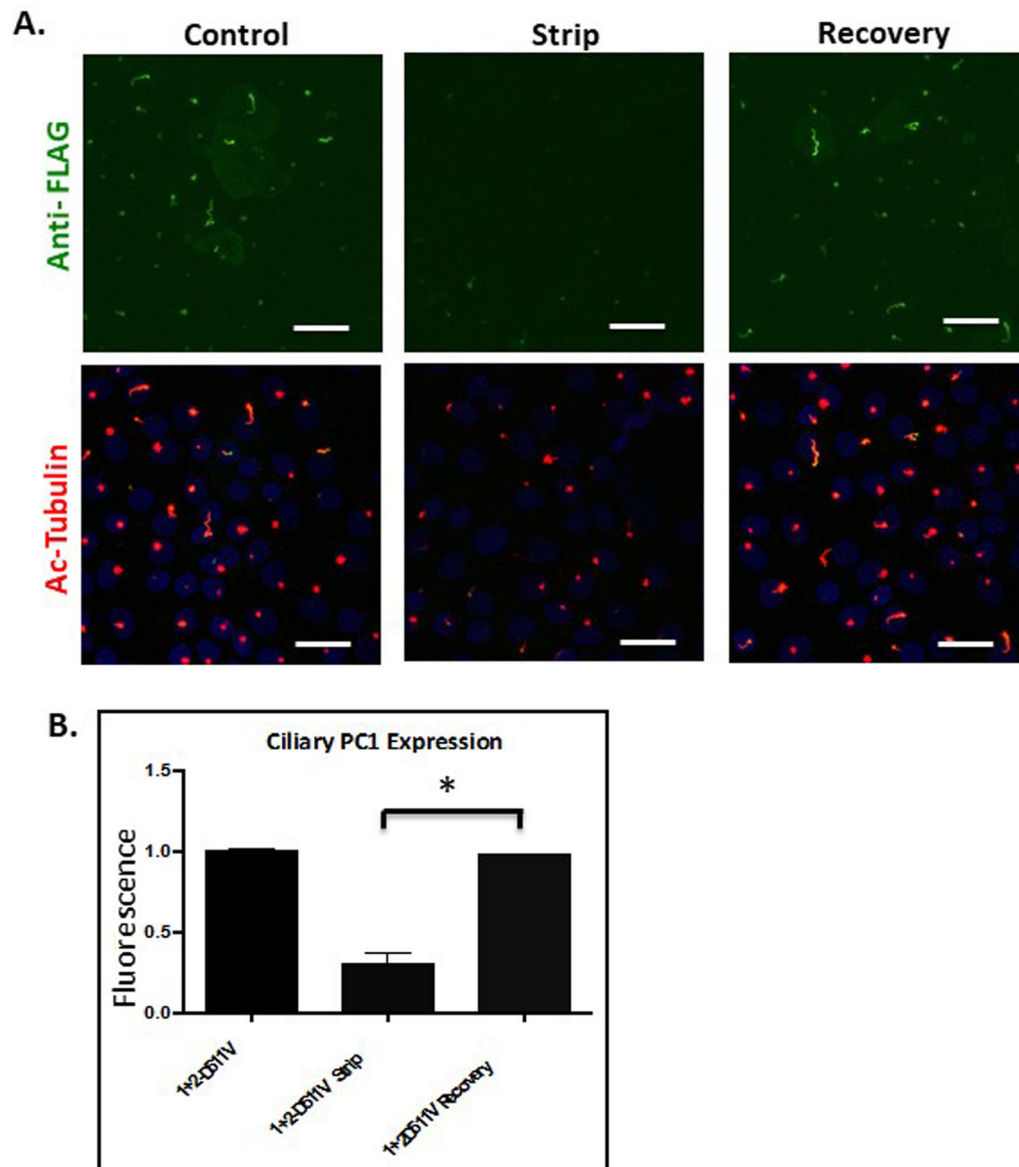


**Figure 5: PC1 delivery to the cilium does not require PC2 channel activity.**

A Strip-Recovery was performed in an LLC-PK1 cell line expressing WT PC1 and PC2-D511V, a PC2 channel defective mutant. B Quantification of Strip-Recovery shows PC1 recovery to cilia comparable to that observed in cells expressing PC1 and wild type PC2. (\*  $p < 0.003$ ) All scale bars correspond to 25  $\mu$ . N=3



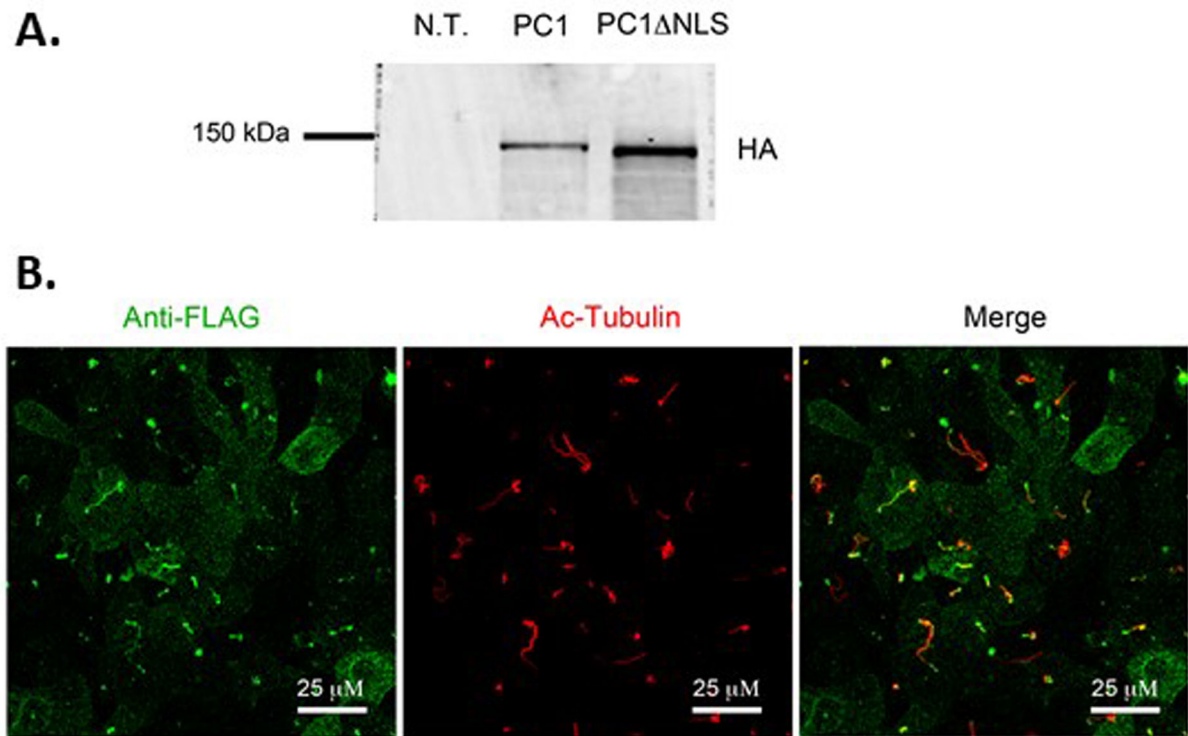


**Figure 6: The NLS is not required for PC1 ciliary localization.**

**A** Western blot analysis of lysates from LLC-PK1 cells expressing PC1 NLS and PC2 using an anti-HA antibody shows that PC1 NLS is cleaved at the GPS site to produce the 150 kDa CTF. **B** Surface immunofluorescence using an anti-Flag antibody to detect the extracellular Flag epitope on the N-terminus of PC1 NLS reveals ciliary localization of this mutant protein, as shown by co-localization with the ciliary marker acetylated tubulin. All scale bars correspond to 25  $\mu$ .

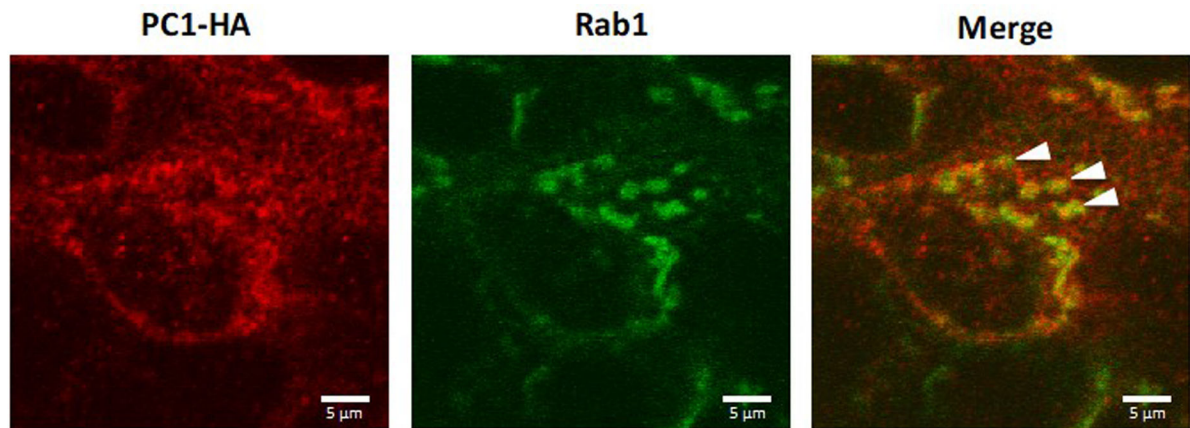


**Figure 7: PC1 partially co-localizes with Rab1a.**

LLC-PK1 cells stably expressing PC1, PC2 and GFP-tagged Rab1a were permeabilized and labeled for immunofluorescence using the anti-HA antibody. The GFP signal marking the Rab1a-positive trafficking compartment partially co-localized with PC1 (arrowheads). All scale bars correspond to 5  $\mu$ .